AIP | Journal of Applied Physics

Experimental evidences of the conservation of the S=1 moment in La2RuO5 determined by perturbed angular correlations

I. B. P. Soares, L. B. Carvalho, J. A. H. Coaquira, G. A. Cabrera-Pasca, A. W. Carbonari et al.

Citation: J. Appl. Phys. **112**, 063915 (2012); doi: 10.1063/1.4754446
View online: http://dx.doi.org/10.1063/1.4754446
View Table of Contents: http://jap.aip.org/resource/1/JAPIAU/v112/i6
Published by the American Institute of Physics.

Experimental evidences of the conservation of the S = 1 moment in La_2RuO_5 determined by perturbed angular correlations

I. B. P. Soares,[1] L. B. Carvalho,[2] J. A. H. Coaquira,[1,a)] G. A. Cabrera-Pasca,[3] A. W. Carbonari,[3] and S. K. Malik[4]
[1]*Núcleo de Física Aplicada, Institute of Physics, University of Brasília, 70904-970 Brasília-DF, Brazil*
[2]*Faculdade Gama-FGA, Sector Central Gama, University of Brasília, 72405-610 DF, Brazil*
[3]*Instituto de Pesquisas Energéticas e Nucleares, IPEN-CNEN/SP, 05508-000 São Paulo, Brazil*
[4]*Departamento de Física Teórica e Experimental, Universidade Federal do Rio Grande do Norte, 59078-400 Natal-RN, Brazil*

(Received 18 January 2012; accepted 24 August 2012; published online 25 September 2012)

A study of the magnetic, electrical resistivity and hyperfine properties of polycrystalline La_2RuO_5 compounds is presented in this work. This compound forms in a monoclinic phase (space group $P2_1/c$). Magnetic susceptibility measurements yield an effective magnetic moment which is consistent with spin $S = 1$ of Ru ions, and a negative paramagnetic Curie temperature which indicates the presence of antiferromagnetic interactions. Below $T \sim 165$ K, the magnetization shows a sudden decrease, precisely where the electrical resistivity shows a change in the activation energy. Room-temperature perturbed angular correlation spectrum is well fitted considering two electric-quadrupole components. The temperature dependences of electric-quadrupole frequencies and asymmetry parameters corroborate the occurrence of a phase transition at $T \sim 170$ K. Moreover, below 170 K, magnetic-dipole interactions, which coexist with electric-quadrupole interactions, are observed at Ru sites. This is considered as a strong evidence for the preservation of $S = 1$ moment of Ru ions in the triclinic phase. The temperature dependence of the magnetic hyperfine field shows an unusual behavior, not consistent with the Brillouin function, and suggests a first-order magnetic transition, associated with either a structural transition or an orbital ordering induced by the Ru-Ru pair formation. [http://dx.doi.org/10.1063/1.4754446]

I. INTRODUCTION

The magnetic behavior of transition metal oxides is generally governed by exchange interactions between metal ion spins. This interaction can occur either via a non-magnetic oxygen ion (super-exchange) or by the direct metal-metal ion interaction (double exchange). On the other hand, electrical and electronic properties of transition metal oxides are commonly understood on basis of the Mott-Hubbard model.[1] Within the framework of this model, the ratio of the strength of intra-ionic Coulomb repulsion between electrons (U) to the conduction band width (W), originating from the overlap of d and p orbitals,[1] is a determinant parameter. For a system where $U/W >> 1$, the splitting of the lower and upper Hubbard band is large and an insulating behavior is expected, while a metallic behavior is expected for $U/W << 1$. A borderline between metal and insulator is expected when $U/W \approx 1$, and this is strongly affected by small perturbations (such as strain, doping, etc.) promoting a metal-insulator transition.[2,3]

The ruthenates (4d transition-metal oxides) are one of the most intriguing systems and exhibit a variety of interesting properties. These include an unconventional superconducting behavior, as observed in Sr_2RuO_4,[4] high T_C itinerant metallic ferromagnetism in $Sr_4Ru_3O_{10}$,[5] and in $SrRuO_3$,[6] normal Fermi-liquid behavior in $La_3Ru_3O_{11}$,[7] a non-Fermi-liquid behavior in $La_4Ru_6O_{19}$,[7,8] and in $Ca_xSr_{1-x}RuO_3$ system with $x > 0.75$,[9] etc. In addition, there are ruthenates which exhibit metal-insulator transition induced by doping (such as in $Sr_3Ru_2O_7$)[10,11] or poor metal behavior, where the coexistence of quasi-2D perovskite-like layers and 1D rutile-type slabs is determinant.[12] The more extended nature of the *4d* orbitals (relative to their *3d* counterparts) is expected to considerably enhance the electron-lattice interaction, which may be the reason for the formation of a variety of structures (ranging from perovskites to pyrochlores) and also should be the source of structural phase transitions caused by metal ion substitutions.[13] This higher degree of delocalization of *4d* orbitals also tends to produce a greater overlap between them, leading to the decrease of the intra-ionic Coulomb interaction in 4*d*-metal oxides compared to the 3*d* counterparts.[14,15]

Recently, interest in 4d-oxides has centered on the novel ruthenate La_2RuO_5 which shows a quasi-two dimensional structure and a first-order structural transition at $T_s \approx 160$ K.[16,17] At high temperatures (above T_s), this compound shows a monoclinic structure (space group $P2_1/c$). Upon cooling, a phase transition from the monoclinic to a triclinic structure (space group $P\bar{1}$) is observed.[18] This transition is accompanied by an unusual 4d-orbital ordering and spin-gap opening. In addition, strong changes have been observed in the magnetic properties by cooling the system below T_s. These results have been attributed to a transition

a)Author to whom correspondence should be addressed. Electronic mail: coaquira.ja@gmail.com.

from the usual $t_{2g\uparrow}^3 t_{2g\downarrow}^1$ low spin state of Ru ions with S = 1 to $t_{2g\uparrow}^2 t_{2g\downarrow}^2$ ultralow spin state with S = 0, which is thought to be caused by the lattice distortions introduced by the structural transition.[16] On the other hand, theoretical studies based on density functional and Hubbard U band structure calculations suggest that the crystal fields occurring in the low temperature phase are not strong enough to stabilize the S = 0 state.[19,20] It means that the orbital ordering happening in the low-temperature phase preserves the magnetic moments of Ru ions and the unusual magnetic behavior is related to the formation of spin ladders (dimers), where the spins S = 1 are antiferromagnetically coupled along the rungs.[20] Although the x-ray absorption spectroscopy measurements reported in Ref. 20 are consistent with the S = 1 state in the low-temperature phase, no direct evidence about the local magnetic state of Ru ions has been experimentally determined. Heat capacity measurements on La_2RuO_5 did indicate an entropy change consistent with S = 1 ground state at low temperatures.[17] Recently, using muon-spin rotation technique, a study of the local magnetic properties of polycrystalline La_2RuO_5 has been carried out.[21] Results suggest the absence of a long-range magnetic order below the transition temperature, while the relaxation effects are consistent with the dimerization of Ru^{4+} ions.

In this work, we present the results of structural, magnetic and electrical resistivity measurements on a polycrystalline sample of La_2RuO_5. Hyperfine properties, determined from perturbed angular correlation (PAC) spectroscopy study, strongly suggest that the S = 1 spin state of Ru^{4+} ions is preserved in the low-temperature phase.

II. EXPERIMENTAL DETAILS

The La_2RuO_5 compound was synthesized from La_2O_3 (99.9%) and RuO_2 (99.95%) using conventional solid-state reaction technique. Stoichiometric amounts of La_2O_3 and RuO_2 were mixed intimately in isopropyl alcohol and dried at ~50 °C. The dried mixture was pressed into pellets under a pressure of $\sim 4 \times 10^7$ kg/m^2 and sintered in air at 1150 °C in an alumina crucible for 36 h. Two heating rates, namely, 2 K/min and 10 K/min have been used to prepare the samples labeled as IS3 and IS8, respectively. Intermediate grindings were performed in order to ensure homogeneity of the samples. Phase characterization and crystal structure determination were carried out by x-ray diffraction (XRD) using Cu-K_α radiation. Magnetic measurements in a temperature range of 5 to 300 K and in magnetic fields up to 7 T were carried out using a commercial vibrating sample magnetometer (VSM). DC resistance measurements were carried out on a piece of sample cut in a rectangular bar shape with dimensions $1.5 \times 3.5 \times 6.0$ mm^3 using a low current of I = 50 nA in order to reduce any significant self-heating at low temperatures. In order to perform PAC measurements and to facilitate the radioactive probe diffusion, the sample powders were pressed into small pellets. A solution containing approximately 20 μCi of carrier-free ^{111}In in the form of indium chloride was dropped on a pellet and slowly evaporated to dryness. Subsequently, the pellet was sealed in a quartz ampule under vacuum and sintered at 1000 °C for 20 h.

The intermediate state of 245 keV and spin $5/2^+$ of the well-known 171–245 keV $\gamma - \gamma$ cascade of ^{111}Cd probe nuclei have been used to measure the hyperfine interactions by PAC spectroscopy. A standard setup with four BaF_2 detectors arranged in a planar 90°–180° geometry and generating simultaneously 12 delayed coincidence spectra has been used. The detector system had a time resolution of 800 ps. The PAC spectra were obtained in a wide temperature range (15–295 K) using a closed-cycle helium refrigeration system.

The PAC method is based on the observation of hyperfine interaction of nuclear moments with an extra nuclear magnetic field (B_{hf}) or an electric field gradient. The technique measures the time evolution of the gamma-ray emission pattern caused by hyperfine interactions. A detailed description of the method as well as details about the PAC measurements can be found elsewhere.[22,23] In PAC technique, the measured perturbation function of polycrystalline systems can be given by

$$R(t) = A_{22} G_{22}(t) = A_{22} \sum_i f_i G_{22}^i(t), \qquad (1)$$

where A_{22} is the unperturbed angular correlation coefficient, f_i are the fractional site populations, and $G_{22}^i(t)$ are the corresponding perturbation factor. Experimentally, the perturbation function is defined as $R(t) = 2\left[\frac{C(180^o,t) - C(90^o,t)}{C(180^o,t) + 2C(90^o,t)}\right]$, where $C(\theta,t)$ is the geometric average of the coincidences obtained from the background subtracted spectra recorded at angle θ.

The perturbation factor $G_{22}(t)$ contains detailed information about the hyperfine interaction between the probe nuclei and the local distribution of electronic charge and spins in their neighborhood. Experimental measurements of $G_{22}(t)$ permit, in the case of pure electric quadrupole interaction, the determination of the spin-independent quadrupole frequency, defined by $\nu_Q = eQV_{zz}/h$, and the asymmetry parameter $\eta = (V_{xx} - V_{yy})/V_{zz}$, where V_{xx}, V_{yy} and V_{zz} are the non-vanishing components of the electric field gradient (EFG) tensor in the principal-axis system, Q is the nuclear quadrupole moment (Q = 0.83 b) of the intermediate nuclear level in the ^{111}Cd probe nucleus. Usually, V_{zz} is the largest component of the EFG tensor. For pure dipole magnetic interaction, the Larmor frequency $\omega_L = g\mu_N B_{hf}/\hbar$ can be deduced from the measured $G_{22}(t)$. By knowing the g factor value (g = 0.31) of the intermediate level of ^{111}Cd, the magnetic hyperfine field at the probe nuclear sites can be determined. Effects of finite time resolution (τ_R) of detectors and the distribution of EFG are properly taken into account in the perturbation function by multiplying G_{22}(t) with the exponential factor of τ_R and the distribution width δ. However, at temperatures below the Néel temperature, the probe nuclei feel magnetic and electric fields and the perturbation function require a combined magnetic-dipole and electric-quadrupole interactions to be considered.

III. RESULTS AND DISCUSSION

A. Crystal structure

The x-ray diffraction data of polycrystalline La_2RuO_5 samples were analyzed using the Rietveld refinement

method. The analysis revealed the formation of a monoclinic structure (space group: $P2_1/c$, #14) at room temperature. As shown in Figure 1, a good fit to the x-ray data is obtained using the starting parameters taken from Ref. 24. Some additional reflections (see inset in Fig. 1) are observed on modifying the sample's preparation conditions. These extra reflections most likely belong to the phase $La_{3.5}Ru_4O_{13}$ which most intense peak matches with the impurity peak and provides a phase concentration of ≈2%, in comparison to the main ruthenate phase. The refined lattice parameters are a = 9.1886(1) Å, b = 5.8294(1) Å and c = 7.9578(1) Å, and $\beta = 100.776°$. These values are in good agreement with those reported in the literature.[18,24]

Further analysis of the x-ray data indicates that the in-plain octahedral Ru-O bond distances are in the range of 1.91-2.17 Å and those parallel to the c axis are ~2.04 Å. The O-Ru-O angles range from ~81° to ~94° and reveal distorted RuO_6 octahedra. Besides that, a next nearest Ru-Ru distance of 3.985 Å is determined. The RuO_6 octahedra are corner-shared through O atoms and form a double-layered perovskite-type structure along the [001] direction (i.e., parallel to the c axis). A zigzag-like pattern of RuO_6 octahedra is formed in the *a-b* plane. These octahedral are separated by LaO layers in the c-direction as depicted in Figure 2(a). The crystal structure of La_2RuO_5 seems to be unique among the isostructural R_2RuO_5 (R = Pr-Tb) compounds.[13] The latter family forms in another orthorhombic structure (space group *Pnma*), instead of a monoclinic structure as La_2RuO_5 does. Because of this, La_2RuO_5 and R_2RuO_5 (R = Pr-Tb) compounds show differences in their magnetic and electric behaviors. Moreover, considering the number of perovskite slabs, La_2RuO_5 is more similar to the n = 2 member of the so-called [110]-phases ($A_nB_nO_{3n+2}$), where zigzag chains of BO_6 octahedra are isolated by A-O units.[18] Although, the n = 2 Ruddlesden-Popper phase compounds, such as $Sr_3Ru_2O_7$, are also built from double perovskite slabs, they show important differences in their connectivities as pointed out in Refs. 16 and 18. This could impart specific electronic properties to the La_2RuO_5 compound.

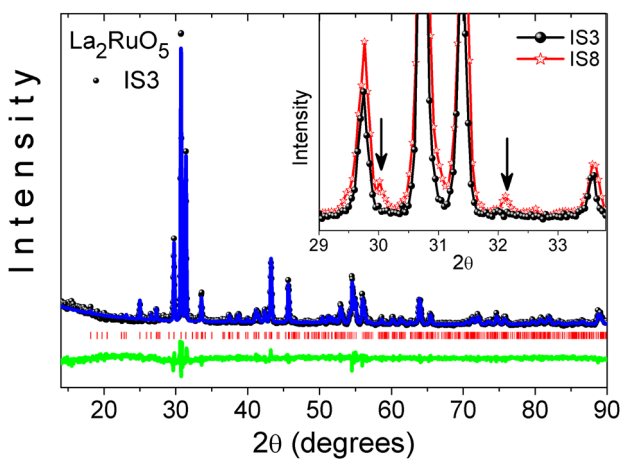

FIG. 1. XRD patterns of La_2RuO_5 compound (IS3) obtained at room temperature. Observed and calculated intensities are represented by closed circles and solid line, respectively. Differences are shown at the bottom part of the figure and vertical tick marks represent the positions of Bragg reflections. The inset shows the extra reflections observed in a sample prepared on modifying the preparation conditions (IS8). See text for details of samples labeled IS3 and IS8.

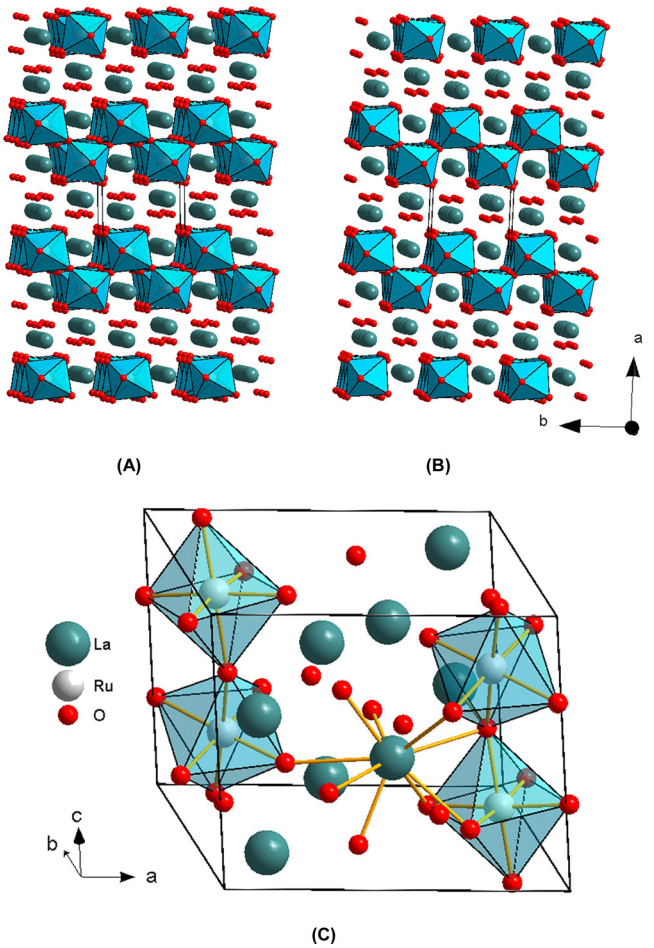

FIG. 2. (a) Representation of the monoclinic crystal structure of La_2RuO_5 projected on the crystallographic *ab* plane. (b) Representation of the triclinic crystal structure of La_2RuO_5 projected on the crystallographic *ab* plane. Dark grey regions represent RuO_6 octahedra. (c) A three-dimensional representation of the triclinic structure, where the coordination number of Ru ions and one La ion is shown.

Accordingly to Khalifah *et al.*,[16] the low-temperature triclinic phase of La_2RuO_5 remains very similar to the high-temperature monoclinic phase, as depicted in Figure 2(b), despite change in space group symmetry. This change in symmetry increases the number of inequivalente sites of Ru (La) ions from one (two) to two (four) as the structure goes from the high- to the low-temperature phase.[18] Moreover, the specific changes in the nature of the Ru-O interactions by going from monoclinic to triclinic structure, such as the formation Ru dimers, must be responsible for the special properties shown by La_2RuO_5 as discussed in Secs. III B and III C.

B. Magnetic and electric properties

Figure 3 shows the temperature (T) dependence of the dc magnetization (M) of La_2RuO_5, obtained in a field of H = 10kOe. At temperatures above 190 K, the magnetic susceptibility shows a behavior well described by the Curie-Weiss law ($\chi = \chi_0 + C/[T - \theta]$). From the analysis of χ vs. T data, an effective paramagnetic moment $\mu_{eff} = (2.74 \pm 0.03)\ \mu_B$ and a paramagnetic Curie-Weiss

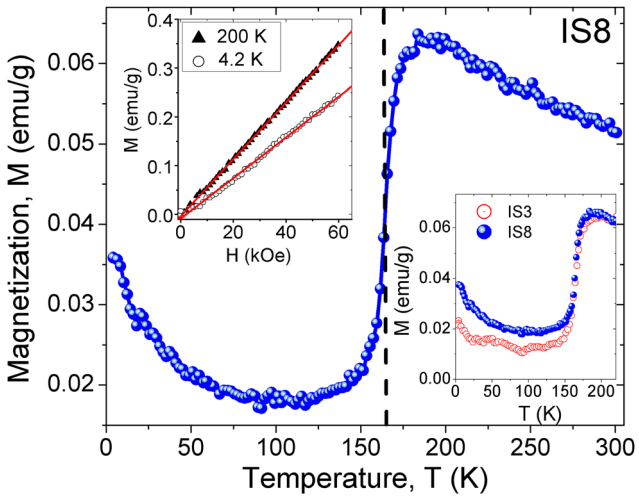

FIG. 3. Temperature dependence of the magnetization of La_2RuO_5 compound obtained in a field of 10 kOe. The inset at the bottom right shows the effect of the impurity phase (sample IS8). The inset at the top left shows magnetization as a function of the applied magnetic field.

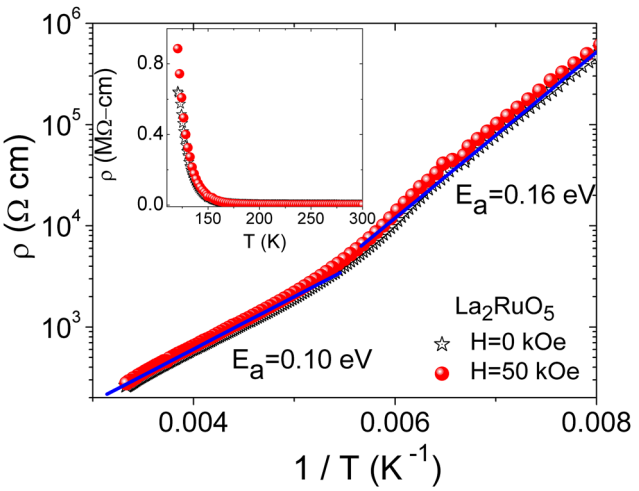

FIG. 4. Electrical resistivity (ρ) of La_2RuO_5 as a function of temperature plotted as lnρ vs. inverse temperature (1/T) in two magnetic fields (H). The inset shows ρ vs. T curve in a linear scale.

temperature $\theta_P = -193 \pm 9$ K are determined. The μ_{eff} value is consistent with a spin S = 1 and confirms the d^4 configuration, i.e., the 4+ oxidation state of ruthenium ions, whereas the sign of θ_P suggests the presence of antiferromagnetic interactions between the Ru spins. As the temperature decreases, the magnetization shows a sudden decrease centered at $T_M = 165 \pm 1$ K. That abrupt change in magnetization is in agreement with reports found in the literature and has been associated with a strong first-order structural transition from the high-temperature monoclinic phase to the low-temperature triclinic phase.[16,17] In the low temperature region, the M vs. T curve shows an upturn when cooling. This upturn is more pronounced for the sample which shows traces of a second phase (sample IS8) as discussed in Sec. III A. This finding suggests that the paramagnetic-like behavior (see the inset at the bottom right of Fig. 3) observed at low temperatures may be related to the extrinsic response of impurity spins.

Figure 4 shows the temperature dependence of the electrical resistivity ($\rho(T)$) in magnetic field of H = 0 and 50 kOe. No remarkable differences between both ρ *vs.* *T* curves are observed over the entire temperature range. Despite the black color of the samples, the negative temperature derivative of the electrical resistivity ($d\rho/dT < 0$) indicates a nonmetallic (semiconducting) behavior in the whole temperature range. The *ln*ρ *vs* 1/*T* plot indicates that the structural transition separates two semiconducting regimes with two different Arrhenius activation energies as shown in the main panel of Figure 4. Above ~170 K, an activation energy $E_a = 0.16$ eV is estimated and this decreases to $E_a = 0.10$ eV when the sample is cooled below 170 K. These activation energies remain essentially the same even when magnetic field is applied. Although, these activation energies are slightly smaller than those reported in the literature for La_2RuO_5 single crystal and sintered pellets,[16] the prominent change in the behavior of resistivity suggests a discrete transition between the two distinct electronic states. As mentioned above, despite the change in space group symmetry, the structural changes related to the monoclinic to triclinic phase transition are found to be very small in this compound.[18] It suggests that the electronic transition is driven by specific changes in the extent of the Ru-O interactions. A systematic study of the nature of the electronic conducting mechanisms above and below the structural transition and its relation to the orbital ordering is currently under investigation and the results will be published elsewhere.[25]

C. Hyperfine interactions

PAC spectra measured at various temperatures are shown in Figure 5. Additionally, in Figure 6, two PAC

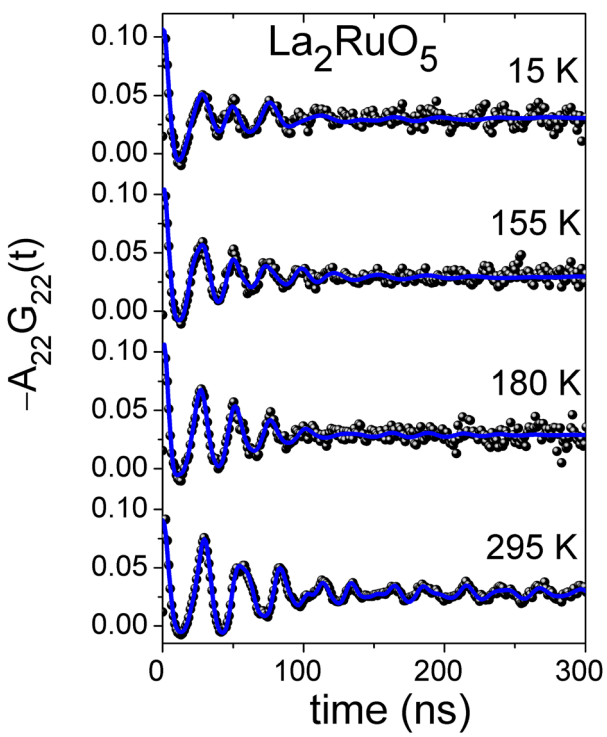

FIG. 5. Perturbed angular correlation spectra of the ^{111}Cd probe in La_2RuO_5 obtained at different temperatures. The solid points represent the experimental data and the solid line is the calculated data.

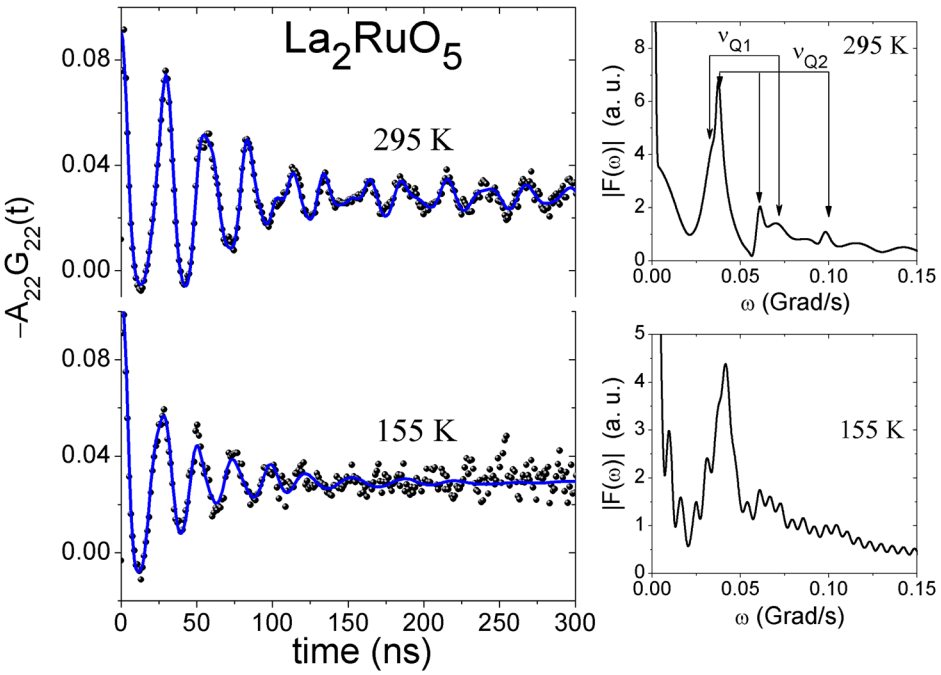

FIG. 6. Perturbed angular correlation spectra of the ^{111}Cd probe in La_2RuO_5 obtained at temperatures above and below the transition temperature. The solid line is the calculated data and the solid points are the experimental data. Plots at the right represent their respective Fourier transforms.

spectra and their respective Fourier transforms measured at 295 K and 155 K are also shown. The experimental data are least-square fitted to the theoretical perturbation function R(t) considering two probe sites. In the Fourier transform plot of the 295 K perturbation function, the indicated peaks represent two sets of frequencies that correspond to two electric-quadrupolar interactions. The correct identification of the locations of the nuclear probe (which give rise to the observed PAC spectrum) in the crystal lattice is not an obvious task. It has not been possible to distinguish frequencies associated with different inequivalent La (Ru) sites occupied by ^{111}Cd probes. However, based on the results of earlier ^{111}In→^{111}Cd PAC measurements in perovskite-type compounds,[23,26] we assign the lower quadrupole frequency $\nu_Q \sim 133$ MHz as being associated with the ^{111}Cd probes substituting Ru atoms and the higher quadrupole frequency $\nu_Q \sim 208$ MHz as being associated with the ^{111}Cd probes substituting the La atoms. Moreover, the ionic radii of six coordinated neighborhoods are 0.76 Å for Ru^{4+} ions, 1.185 Å for La^{3+} ions, and 0.94 Å for In^{3+} ions. Based on ionic radii considerations, it is expected that the ^{111}In probes substitute both kind of cations, since the differences in radii between ^{111}In probe and both cations are similarly close. Additionally, the larger quadrupole frequency of La sites must be associated with the larger number (nine) of O^{2-} neighbors in contrast to the number of neighboring anions (six) of Ru sites (see Fig. 2(c)), which must lead to lower quadrupole frequency for Ru sites.[24]

Figure 7 shows the temperature dependence of the hyperfine parameters for the two electric-quadrupole interactions. The site occupancy fractions of both sites remain essentially constant over the entire temperature range (15-295 K). The ν_Q related to ^{111}Cd probes occupying La sites shows a smooth decrease as the temperature is decreased across the transition temperature. However, the electric-quadrupole component associated with the ^{111}Cd probes substituting Ru atoms shows an increase as the temperature is decreased until ~190 K. Below that temperature, a combined electric quadrupole and magnetic dipole interactions are determined from the PAC subspectra associated with the Ru sites. Additionally, the quadrupole frequency of ^{111}Cd probes at the Ru sites (ν_Q^{Ru}) shows a sudden decrease at around T ~ 170 K. The region where the sudden change in

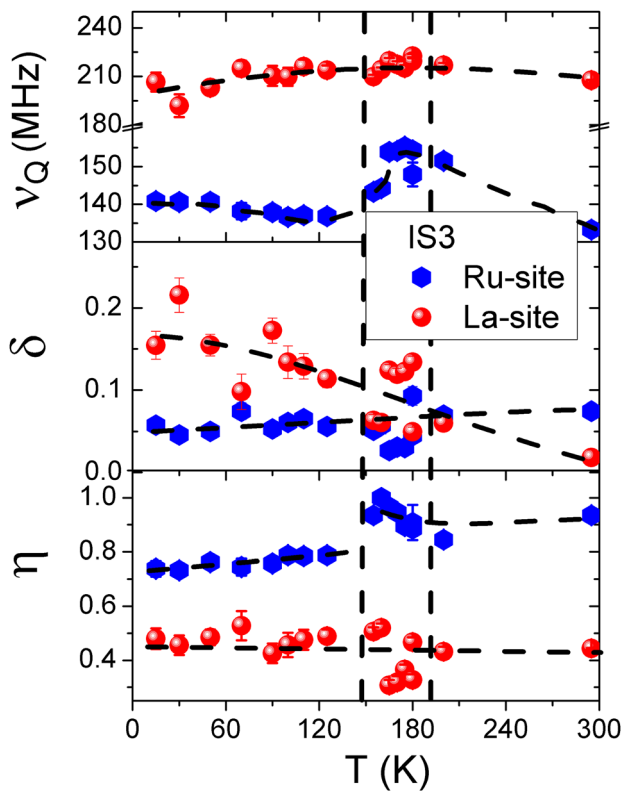

FIG. 7. Temperature dependence of the hyperfine parameters of the ^{111}Cd probes at La and Ru sites in La_2RuO_5. The vertical lines indicate the region of structural transition.

ν_Q^{Ru} is observed coincides with the region where magnetic and electrical resistivity measurements show anomalies, as discussed above. Below ~150 K, a smooth behavior in ν_Q^{Ru} is observed on decreasing the temperature as shown in Fig. 7.

The frequency distribution width (δ) associated with the Ru sites shows a small variation (7-5%) as the temperature is decreased from 295 K towards 15 K, while the distribution width of La sites shows a monotonous increase as the temperature is decreased. This increase becomes more pronounced at temperatures below the structural transition (see Fig. 7). On the other hand, the asymmetry parameter of ^{111}Cd probes at the La sites (η^{La}) remains nearly constant ($\eta^{La} \sim 0.5$), even below the transition temperature; however, η^{Ru} shows a small variation when the temperature is decreased towards ~170 K. Around the transition temperature, η^{Ru} shows a drop from ~0.95 to 0.80 which suggests that the RuO_6 octahedra become less distorted in the low-temperature triclinic phase.

As mentioned above, the magnetic dipole component that appears in the PAC subspectra of Ru sites below 190 K, is represented by the Larmor frequency (ω_L). This frequency is related to the magnetic hyperfine field by: $\omega_L = g\mu_N B_{hf}/\hbar$. Using g = 0.31 for the $I = 5/2^+$ intermediate level of ^{111}Cd and the obtained Larmor frequency ω_L~33 Mrad/s, we estimate a magnetic hyperfine field B_{hf} ~2.3 T from the spectrum obtained at T = 15 K. This magnetic hyperfine field shows the temperature dependence depicted in Figure 8. As seen, this temperature dependence is different from that expected from the Brillouin function, which describes the usual second-order magnetic transitions, and suggests that the transition observed in La_2RuO_5 compound could be rather a first-order type transition, which is supported by the steeper variation of B_{hf} around the magnetic transition ($T_M \sim 165$ K). We believe that this unusual magnetic transition must be intimately related to the structural transition ($T_s \sim 160$ K),[16] since both of them happen almost at the same temperature.

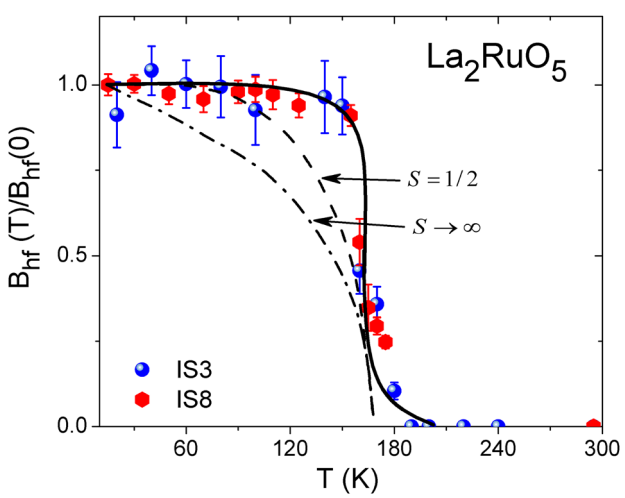

FIG. 8. Normalized magnetic hyperfine field of the ^{111}Cd probes at Ru sites as a function of the temperature. Calculated Brillouin functions (for S = 1/2 and S $\rightarrow\infty$) are included for comparison. The solid line is drawn to guide the eyes.

It is worth noting that, since the ^{111}Cd probe has a closed d-electron shell, no effects of d-electron superexchange is expected and the magnetic hyperfine field determined by PAC measurements is referred only to the transferred hyperfine field (THF). The directional bonding of Ru-O-Ru bonds through corner-shared RuO_6 octahedra provides a direct pathway for that THF at the Ru sites because of the exchange bond angle (~150-160°). In contrast, the exchange angles of the Ru-O-La bonds are in the range of~85-102°, which only produce a small overlap between oxygen *p* orbital and *s* orbital of Cd^{2+} ions and imply a weaker THF at the La sites in comparison to the THF at the Ru sites. Although no THF for the ^{111}Cd probe substituting La sites is determined from our PAC measurements, its presence must not be completely disregarded, since the distribution width (δ) of the electric quadrupole contribution at the La sites shows a monotonous increases as the temperature is decreased. That increase could be a symptom of the occurrence of weak magnetic dipole interactions which coexist with electric quadrupole interactions below ~190 K at the La sites.

The small value of the THF, $B_{hf}^{Cd}(0) \sim 2.3$ T at the Ru sites, must be a consequence of the weak overlap between *d* orbitals of Ru^{4+} and *p* orbitals of O^{2-}. This is supported by the THF of similar order determined for ruthenates with perovskite-type structure from ^{111}In→^{111}Cd PAC measurements.[25] It is know that only t_{2g} (d_{xy}, d_{yz}, d_{zx}) orbitals of Ru^{4+} are expected to be occupied in the low temperature phase.[16,19,20] It implies that e_g orbitals of Ru^{4+} are empty. Therefore, due to the small overlap between t_{2g} orbitals and nearby oxygen ions,[24] these orbitals tend to show localized character and, consequently, transfer a little spin density to Cd^{2+} orbitals via $Ru^{4+} - O^{2-} - Cd^{2+}$ bonds, which produces a small THF at the Cd^{2+} nuclei.

Although the presence of magnetic hyperfine field in La_2RuO_5 does not provide any specific information about the orbital ordering, it clearly reveals the conservation of the spin S = 1 of Ru^{4+} ions through the structural transition. It is known that the orbital degeneracy is lifted by the small structural changes[19,20] coming along with the phase transition below ~170 K. This lifting of orbital degeneracy favors orbital ordering and the formation Ru-Ru pairs, where their spins are oppositely aligned. Although antiferromagnetism has been determined for this ruthenate, its nature is not of long-range order and no magnetic dipole interactions are expected in this system, since all Ru pairs are S = 0 below ~170 K. This finding is in agreement with the study carried out by muon spin rotation technique.[21] However, the substitution of Ru ions by ^{111}Cd probes provides a scenario to measure local magnetic field (which is felt by the ^{111}Cd probes located at Ru sites) produced by the next-nearest Ru ion.

IV. CONCLUSIONS

While the structural data confirm the formation of monoclinic phase at room temperature, the magnetic and electrical measurements on a polycrystalline La_2RuO_5 compound corroborate the structural transition from monoclinic

to triclinic phase happening at $T \sim 165$ K. High-temperature magnetic measurements are consistent with the valence state 4+ of ruthenium ions (i.e., spin $S = 1$), and indicate an antiferromagnetic coupling between the magnetic moments. Below ~165 K, the magnetization results seem to be consistent with the loss of the local magnetic moment induced by the orbital ordering from $t_{2g\uparrow}^3 t_{2g\downarrow}^1$ $(S = 1)$, in the high-temperature monoclinic phase, to $t_{2g\uparrow}^2 t_{2g\downarrow}^2$ $(S = 0)$, in the low-temperature triclinic phase. However, perturbed angular correlation experiments corroborate the occurrence of phase transition at $T \sim 170$ K and provide strong evidences for the preservation of the spin $S = 1$ of Ru^{4+}. This finding is evidenced by the presence of magnetic-dipole interactions which coexist with electric-quadrupole interactions at the Ru sites below ~170 K. The magnetic hyperfine field shows a temperature dependence which seems to be consistent with a first-order transition, likely associated with the structural transition or with the orbital ordering induced by the formation of Ru-Ru pairs.

ACKNOWLEDGMENTS

This work was financially supported by the Brazilian Agencies CNPq, CAPES, and FAPDF. The authors are grateful to Dra. E. M. Guimarães for carrying out x-ray diffraction measurements. The work at UFRN was supported by CAPES through a fellowship to SKM.

[1]Z. Fang and K. Terakura, Phys. Rev. B **64**, 020509(R) (2001).
[2]G. Cao, C. S. Alexander, S. McCall, J. E. Crow, and R. P. Guertin, Mater. Sci. Eng. B **63**, 76 (1999).
[3]M. Z. Cieplak, S. Guha, H. Kojima, P. Lindenfeld, G. Xiao, J. Q. Xiao, and C. L. Chien, Phys. Rev B **46**, 5536 (1992).
[4]Y. Maeno, H. Hashimoto, K. Yoshida, S. Nishizaki, T. Fujita, J. G. Bednorz, and F. Lichtenberg, Nature (London) **372**, 532 (1994).
[5]M. K. Crawford, R. L. Harlow, W. Marshall, Z. Li, G. Cao, R. L. Lindstrom, Q. Huang, and J. W. Lynn, Phys. Rev B **65**, 214412 (2002).
[6]Y. Yoshida, I. Nagai, S.-I. Ikeda, N. Shirakawa, M. Kosaka, and N. Môri, Phys. Rev B **69**, 220411(R) (2004).
[7]P. Khalifah, K. D Nelson, R. Jin, Z. Q. Mao, Y. Liu, Q. Huang, X. P. A. Gao, A. P. Ramirez, and R. Cava, Nature **411**, 669 (2001) and references therein.
[8]P. Khalifah and R. J. Cava, Phys. Rev. B **64**, 085111 (2001).
[9]P. Khalifah, I. Ohkubo, H. M. Christen, and D. G. Mandrus, Phys. Rev. B **70**, 134426 (2004).
[10]A. W. Sleight and J. L. Gillson, Mater. Res. Bull. **6**, 781 (1971).
[11]R. Mathieu, A. Asamitsu, Y. Kaneko, J. P. He, X. Z. Yu, R. Kumai, Y. Onose, N. Takeshita, T. Arima, H. Takagi, and Y. Tokura, Phys. Rev. B **72**, 092404 (2005).
[12]J. A. H. Coaquira, R. L. de Almeida, L. B. de Carvalho, S. Quezado, and S. K. Malik, J. Appl. Phys. **106**, 013909 (2009).
[13]G. Cao, S. McCall, Z. X. Zhou, C. S. Alexander, J. E. Crow, R. P. Guertin, and C. H. Mielke, Phys. Rev. B **63**, 144427 (2001).
[14]G. Cao, S. McCall, M. Shepard, J. E. Crow, and R. P. Guertin, Phys. Rev. B **56**, R2916 (1997).
[15]J. Okamoto, T. Mizokawa, A. Fujimori, I. Hase, M. Nohara, H. Takagi, Y. Takeda, and M. Takano, Phys. Rev. B **60**, 2281 (1999).
[16]P. Khalifah, R. Osborn, Q. Huang, H. W. Zandbergen, R. Jin, Y. Liu, D. Mandrus, and R. J. Cava, Science **297**, 2237 (2002).
[17]S. K. Malik, D. C. Kundaliya, and R. D. Kale, Solid State Commun. **135**, 166 (2005).
[18]S. G. Ebbinghaus, Acta Cryst. C **61**, i96 (2005).
[19]V. Eyert, S. G. Ebbinghaus, and T. Kopp, Phys. Rev. Lett. **96**, 256401 (2006).
[20]H. Wu, Z. Hu, T. Burnus, J. D. Denlinger, P. G. Khalifah, D. G. Mandrus, L. Y. Jang, H. H. Hsieh, A. Tanaka, K. S. Liang, J. W. Allen, R. J. Cava, D. I. Khomskii, and L. H. Tjeng, Phys. Rev. Lett. **96**, 256402 (2006).
[21]S. J. Blundell, T. Lancaster, P. J. Baker, and W. Hayes, F. L. Pratt, T. Atake, D. S. Rana, and S. K. Malik, Phys. Rev. B **77**, 094424 (2008).
[22]A. W. Carbonari, R. N. Saxena, W. Pendl, Jr., J. Mestnik Filho, R. Attili, M. Olzon-Dionysio, and S. D. de Souza, J. Magn. Magn. Mater. **163**, 313 (1996).
[23]R. Dogra, A. C. Junqueira, R. N. Saxena, A. W. Carbonari, J. Mestnik-Filho, and M. Moralles, Phys. Rev. B **63**, 224104 (2001).
[24]P. Boullay, D. Mercurio, A. Bencan, A. Meden, G. Drazic, and M. Kosec, J. Solid State Chem. **170**, 294 (2003).
[25]I. B. P. Soares, J. A. H. Coaquira *et al*. "Electronic conducting mechanisms in La_2RuO_5 and its relation to the orbital ordering induced by the Ru-Ru pair formation" (to be published).
[26]G. L. Catchen, T. M. Rearick, and D. G. Schlom, Phys. Rev. B **49**, 318 (1994).